Effects of the biological backbone on stacking interactions at DNA−protein interfaces: The interplay between the backbone···π and π···π components

Cassandra D. M. Churchill, Lesley R. Rutledge and Stacey D. Wetmore[*]

Department of Chemistry and Biochemistry, University of Lethbridge, 4401 University Drive, Lethbridge, Alberta, Canada T1K 3M4

Electronic Supplementary Information (ESI)

Table of Contents

Quantum Theory of Atoms in Molecules (QTAIM) Discussion

To complement our calculated binding strengths, the quantum theory of atoms in molecules (QTAIM)[1-3] was used to analyze the electron density and identify interactions within our extended model dimers, as well as the individual π···π and backbone···π components. QTAIM was originally shown to be a very useful approach for verifying the presence of hydrogen-bonding interactions,[4] where current work has expanded to other noncovalent interactions (such as π···π stacking and X–H···π (X=N, O, S, C, etc.)).[5-24] Specifically, studies have shown that hydrogen-bonding interactions can be characterized by the presence of bond critical points (BCPs) between hydrogen-bond donor and acceptor sites (sometimes referred to as HBCPs),[4,22] where the electron density ($\rho(r)$) at the HBCP can be related to the hydrogen-bond strength.[6] Additionally, the sum of the electron densities at all HBCPs in complexes involving several hydrogen bonds can be related to the total complex stability.[22] Similarly, it has been proposed that the existence of cage critical points (CCPs) between rings correlated with the phenomenon of π···π stacking interactions,[8] where it has also been suggested that the relative strengths of stacked complexes can be correlated with the electron density $\rho(r)$ and/or the Laplacian of the electron density ($\nabla^2\rho(r)$) at this unique CCP (see, for example, refs. [7-9,17] for further discussion).

In the present work, six representative examples of the extended dimers were investigated using QTAIM: A–HIS (deoxyribose, O4′ side), C–HIS′ (protein backbone), C–PHE (protein backbone), G–TYR (deoxyribose, C2′ side), T–TRP′ (deoxyribose, C2' side) and U–TYR′ (deoxyribose, O4′ side). In all dimers considered, our QTAIM analysis identifies critical points between the biological backbone and the π-system (see Figs. ESI-1c, ESI-2c and ESI-3c). For example, Fig. ESI-1 illustrates the contacts in the C–HIS' (protein backbone), where one bond critical point (BCP) is visible between Hβ of the protein backbone and O2 of cytosine. Additionally, Fig. ESI-3 illustrates U–TYR' (deoxyribose, O4' side) dimers, where two BCPs are identified between O4' in the deoxyribose moiety and H1 or H2 of tyrosine. The presence of these bond paths verifies the existence of backbone···π contacts and supports our conclusion that these discrete backbone···π contacts contribute to the total interaction energy in extended nucleobase-amino acid dimers.

In attempts to determine whether the backbone···π interactions influence the π···π interactions, QTAIM analysis was performed on the individual (π···π and backbone···π) components within the extended model by replacing the biological backbone or ring in the extended model with a hydrogen atom (see, Figs. ESI-1, ESI-2 and ESI-3). Through visual inspection of the molecular graphs, it is clear that additional critical points are present in some extended dimers

compared to the corresponding components. However, Tables 1 – 3 in the text reveal that the presence of these additional critical points does not necessarily correspond to a larger binding strength calculated for the extended model (ΔE_{ext}) compared with that predicted from the components (ΔE_{predic}). For example, for the U–TYR' (deoxyribose, O4' side) dimer, an additional CCP is found in the extended model even though the binding strengths of the truncated models sum to yield a larger binding strength (i.e., $\Delta E_{predic} > \Delta E_{ext}$ by 3.4 kJ mol^{-1}). Furthermore, the sum of the electron densities at the critical points (Table ESI-1) does not correlate with the binding strength. For example, for the U–TYR' (deoxyribose, O4' side) dimer, the $\Delta E_{predic} > \Delta E_{ext}$ trend cannot be explained by the sum of the densities at all CCPs (Table ESI-1), which is larger for the extended model (18.046 x 10^3 au) than the sum of the $\pi\cdots\pi$ and backbone$\cdots\pi$ contributions of the predicted model (8.995 x 10^3 au). This example demonstrates that there is no correlation between the total stability of the extended and predicted complexes and the sum of the densities at the critical points.

There are discrepancies between the total number and/or type of critical points present in the extended and calculated complexes (see Figs. ESI-1, ESI-2, and ESI-3). We note that this discrepancy could be in part due to the fact that as the number of BCPs increase, additional CCPs are enforced by the Poincaré-Hopf relationship.[1-3] Therefore, for example, the presence of more BCPs in the extended model systems leads to the creation of more CCPs compared to the corresponding separated $\pi\cdots\pi$ and backbone$\cdots\pi$ components. Although the Poincaré-Hopf relationship is satisfied for all complexes considered in the present work, this does not guarantee that all critical points were identified,[1-3] which could also partially explain the apparent discrepancy. Nevertheless, our findings suggest that QTAIM provides confirmation that contacts between the biological backbones and rings exist in extended systems. However, due to the small electron densities at BCPs and CCPs in our stacked systems, QTAIM does not provide conclusive relationships between the electron densities ($\rho(r)$) at BCPs and CCPs and the relative strengths of π-interactions in extended and truncated models.

References

1. R. F. W. Bader, *Atoms in Molecules: A Quantum Theory; International Series of Monographs on Chemistry*, Clarendon Press: Oxford, New York, 1990.
2. P. L. A. Popelier, *Atoms in Molecules: An Introduction*, Prentice Hall, London, 2000.
3. C. F. Matta and R. J. Boyd, eds., *The Quantum Theory of Atoms in Molecules: From Solid State to DNA and Drug Design*, Wiley-VCH, Weinheim, 2007.
4. U. Koch and P. L. A. Popelier, *J. Phys. Chem.*, 1995, **99**, 9747–9754.
5. P. Hobza, J. Sponer, E. Cubero, M. Orozco and F. J. Luque, *J. Phys. Chem. B*, 2000, **104**, 6286–6292.
6. S. J. Grabowski, W. A. Sokalski and J. Leszczynski, *J. Phys. Chem. A*, 2005, **109**, 4331–4341.
7. R. Parthasarathi and V. Subramanian, *Structural Chem.*, 2005, **16**, 243–255.
8. O. A. Zhikol, O. V. Shishkin, K. A. Lyssenko and J. Leszczynski, *J. Chem. Phys.*, 2005, **122**, 144104(144108).
9. C. F. Matta, N. Castillo and R. J. Boyd, *J. Phys. Chem. B*, 2006, **110**, 563–578.
10. A. H. Pakiari and S. Fakhraee, *J. Theor. Comput. Chem.*, 2006, **5**, 621–631.
11. D. Quinonero, A. Frontera, C. Garau, P. Ballester, A. Costa and P. M. Deya, *ChemPhysChem*, 2006, **7**, 2487–2491.
12. M. Ziolkowski, S. J. Grabowski and J. Leszczynski, *J. Phys. Chem. A*, 2006, **110**, 6514–6521.
13. A. Frontera, D. Quinonero, A. Costa, P. Ballester and P. M. Deya, *New J. Chem.*, 2007, **31**, 556–560.
14. D. Escudero, A. Frontera, D. Quinonero and P. M. Deya, *Chem. Phys. Lett.*, 2008, **456**, 257–261.
15. D. Quinonero, A. Frontera, D. Escudero, P. Ballester, A. Costa and P. M. Deya, *Theor. Chem. Acc.*, 2008, **120**, 385–393.
16. A. Ebrahimi, M. Habibi, R. S. Neyband and A. R. Gholipour, *Phys. Chem. Chem. Phys.*, 2009, **11**, 11424–11431.
17. A. Ebrahimi, M. Habibi-Khorassani, A. R. Gholipour and H. R. Masoodi, *Theor. Chem. Acc.*, 2009, **124**, 115–122.
18. D. Escudero, C. Estarellas, A. Frontera, D. Quinonero and P. M. Deya, *Chem. Phys. Lett.*, 2009, **468**, 280–285.
19. C. Estarellas, A. Frontera, D. Quinonero, I. Alkorta, P. M. Deya and J. Elguero, *J. Phys. Chem. A*, 2009, **113**, 3266–3273.
20. C. Estarellas, A. Frontera, D. Quinonero and P. M. Deya, *Chem. Phys. Lett.*, 2009, **479**, 316–320.
21. L. Estevez, N. Otero and R. A. Mosquera, *J. Phys. Chem. A*, 2009, **113**, 11051–11058.
22. S. M. LaPointe, S. Farrag, H. J. Bohorquez and R. J. Boyd, *J. Phys. Chem. B*, 2009, **113**, 10957–10964.
23. A. D. Yau, E. F. C. Byrd and B. M. Rice, *J. Phys. Chem. A*, 2009, **113**, 6166–6171.
24. L. R. Rutledge, C. D. M. Churchill and S. D. Wetmore, *J. Phys. Chem. B*, 2010, **114**, 3355–3367.

(a)
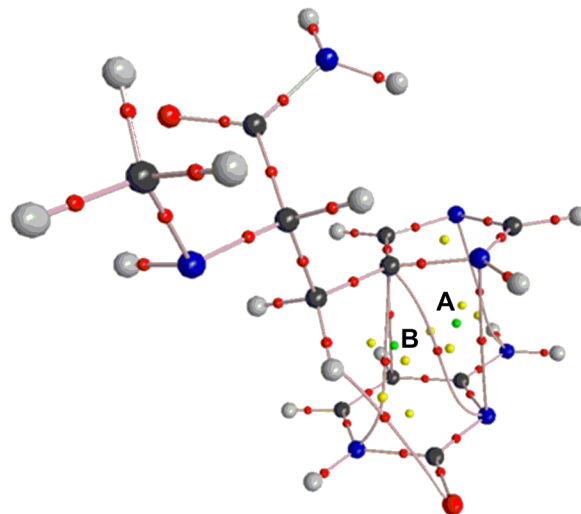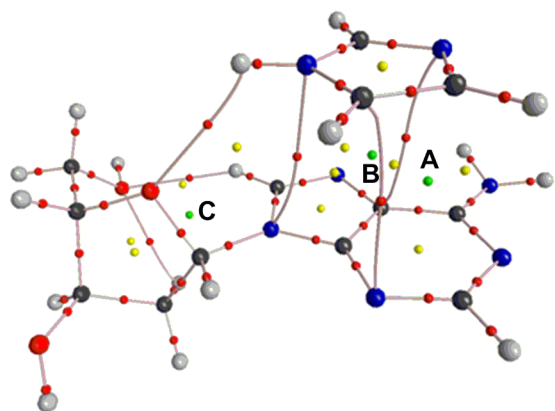
(b)
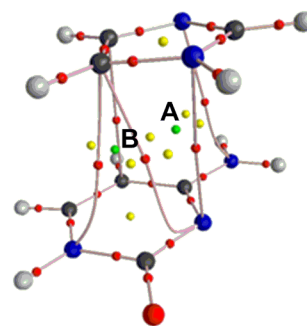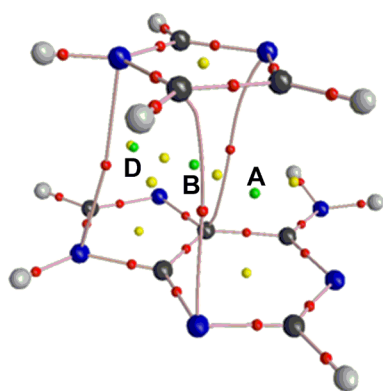
(c)
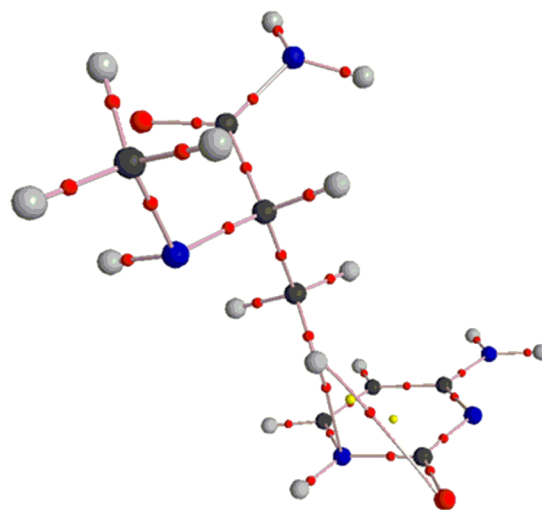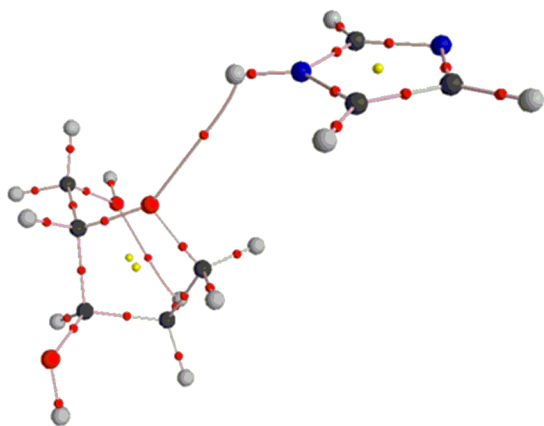
Fig. ESI-1 QTAIM molecular graphs for the (a) A–HIS extended deoxyribose dimer with the amino acid on the O4′ side (left) and C–HIS′ extended protein backbone dimer (right), as well as the corresponding individual (b) π···π and (c) backbone···π contributions. Cage critical points are indicated by a capitol letter (A, B, C or D).

(a)

(b)

(c)
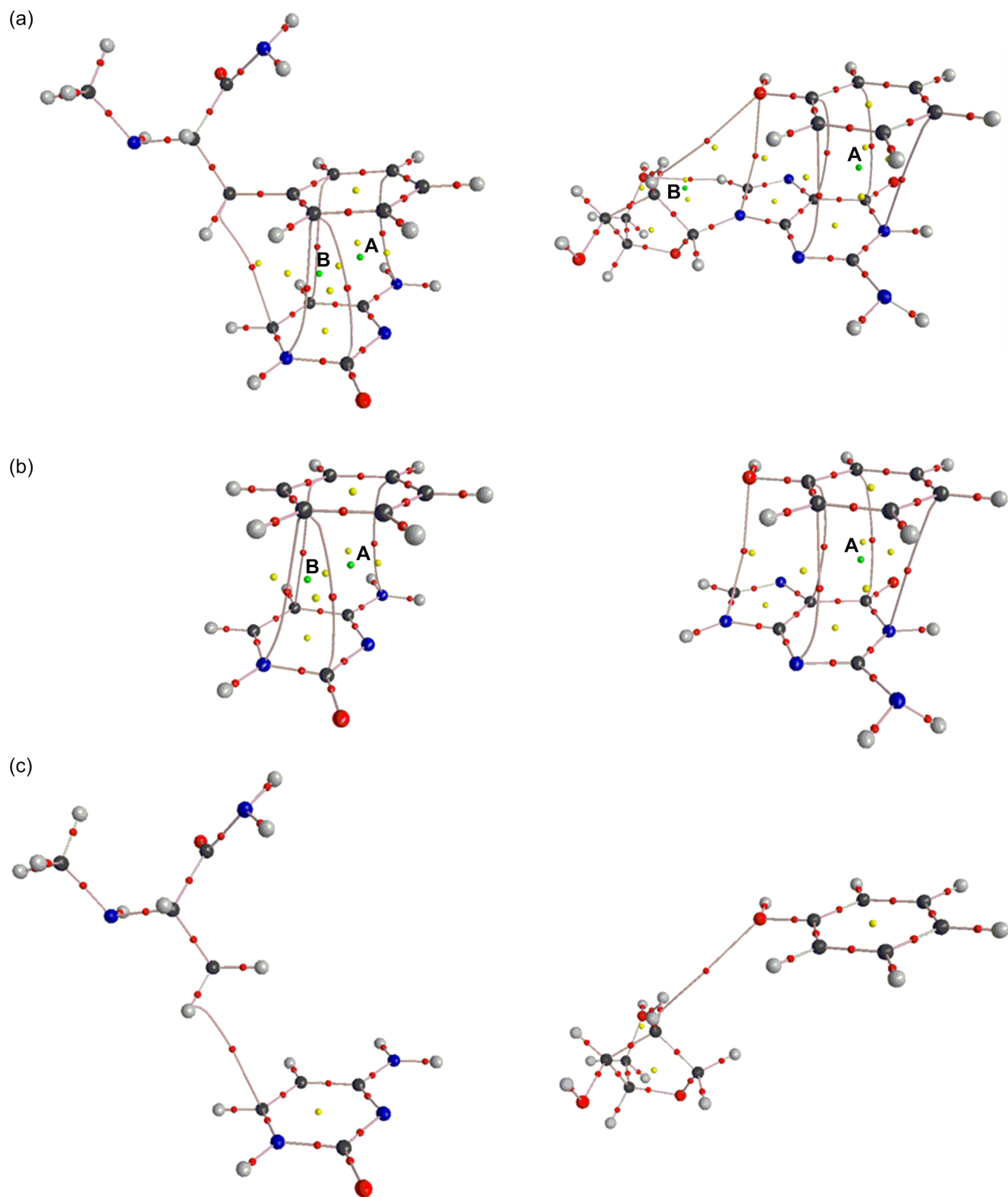
Fig. ESI-2 QTAIM molecular graphs for the (a) C–PHE extended protein backbone dimer (left) and G–TYR extended deoxyribose dimer with the amino acid on the C2′ side (right), as well as the corresponding individual (b) π···π and (c) backbone···π contributions. Cage critical points are indicated by a capitol letter (A or B).

(a)

(b)

(c)
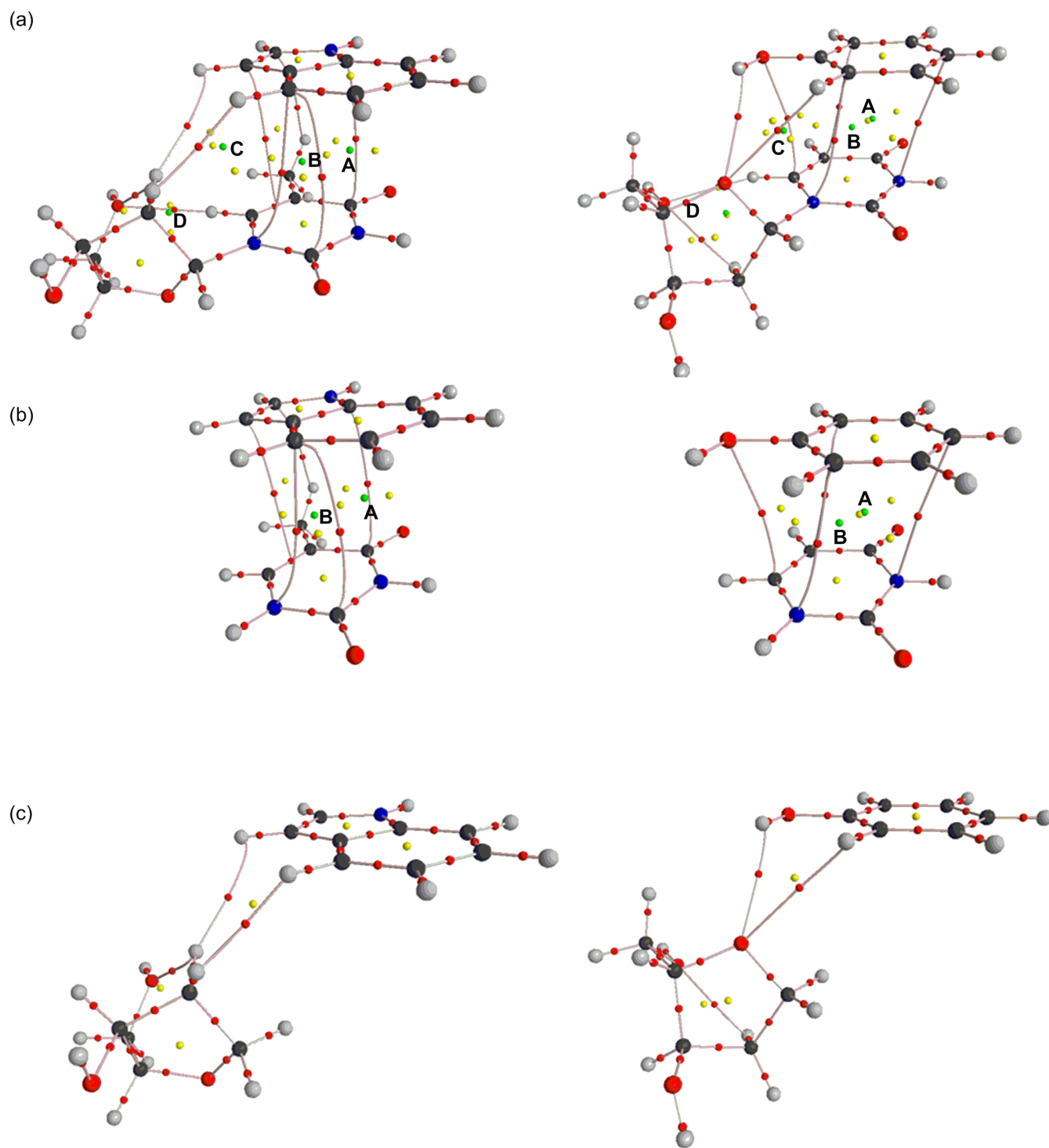
Fig. ESI-3 QTAIM molecular graphs for the (a) T–TRP′ extended deoxyribose dimer with the amino acid on the C2′ side (left) and U–TYR′ extended deoxyribose dimer with the amino acid on the O4′ side (right), as well as the corresponding individual (b) π⋯π and (c) backbone⋯π contributions. Cage critical points are indicated by a capitol letter (A, B, C or D).

(a)

(b)
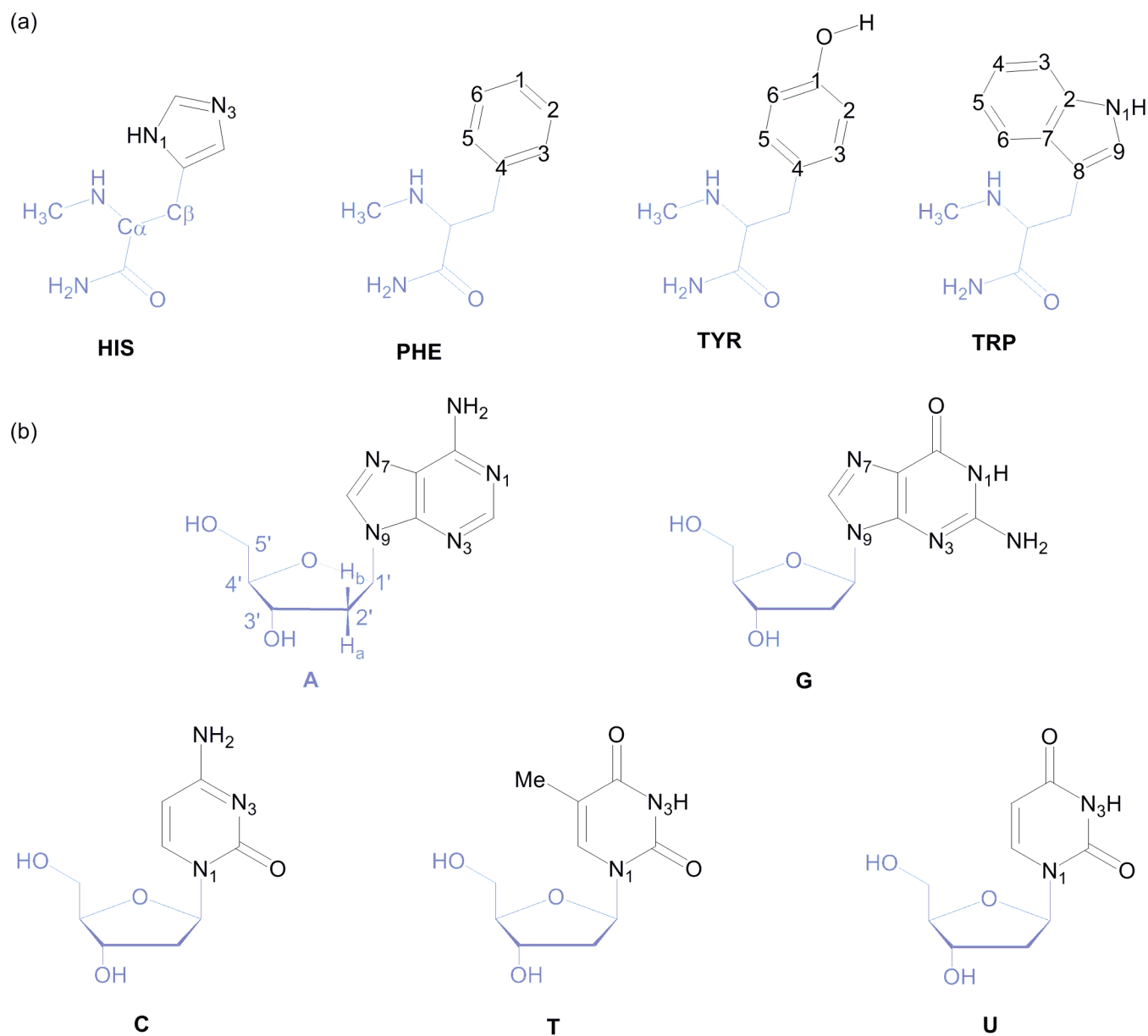
Fig. ESI-4 Structure of (a) the aromatic amino acids (histidine (HIS), phenylalanine (PHE), tyrosine (TYR) and tryptophan (TRP)) and (b) the natural bases (adenine (A), cytosine (C), guanine (G), thymine (T) and uracil (U)) and the full atomic numbering used to discuss QTAIM results.

8

Table ESI-1 Charge density (ρ (r), au), Laplacian (^{2}ρ(r), au) and their variation (Δ ρ (r) and Δ(^{2}ρ(r))) at critical points occurring in select extended models, as well as their individual π ···π and backbone···π components.

Model	Component	CP	Atoms[a]	Extended ρ (r) (×10³)	Extended ²ρ(r) (×10²)	Calculated ρ (r) (×10³)	Calculated ²ρ(r) (×10²)	Variation Δ ρ (r) (×10³)	Variation Δ(²ρ(r)) (×10²)
A–HIS 2'- deoxyribose O4'-side	π···π	BCP	N9–N1	7.246	2.251	7.381	2.218	−0.136	0.033
		BCP	C5–N3	7.693	2.390	7.709	2.392	−0.016	−0.003
		BCP	N3–C5	8.019	2.158	8.023	2.158	−0.004	0.000
		CCP	A	4.956	2.054	4.952	2.056	0.004	−0.002
		CCP	B	5.352	2.253	5.382	2.252	−0.030	0.000
		CCP	D	–	–	5.335	2.142	−5.335	−2.142
	bb···π	BCP	O4'–H1	5.022	2.090	4.981	2.080	0.040	0.010
		CCP	C	4.286	1.944	–	–	4.286	1.944
C–HIS' protein backbone	π···π	BCP	N1–N1	5.578	1.892	5.641	1.888	−0.064	0.004
		BCP	N6–N3	5.576	1.784	5.596	1.786	−0.019	−0.002
		BCP	C5–C4	6.035	1.685	6.071	1.680	−0.035	0.004
		BCP	N3–C5	5.451	1.729	5.722	1.692	−0.271	0.037
		BCP	N1–C5	5.512	1.901	5.614	1.952	−0.102	−0.051
		CCP	A	4.790	2.026	4.819	2.015	−0.029	0.012
		CCP	B	4.380	1.675	4.424	1.706	−0.044	−0.030
	bb···π	BCP	N3–Cβ	–	–	3.868	1.312	−3.868	−1.312
		BCP	O2–Hβ	4.072	1.634	4.076	1.592	−0.003	0.041
C–PHE protein backbone	π···π	BCP	N1–C2	3.900	1.222	3.978	1.222	−0.077	−0.001
		BCP	C2–C2	3.846	1.354	3.874	1.375	−0.027	−0.022
		BCP	N4–C5	4.432	1.303	4.441	1.308	−0.009	−0.005
		BCP	C5–C6	4.718	1.249	4.825	1.250	−0.107	−0.002
		CCP	A	2.886	1.262	2.891	1.264	−0.005	−0.002
		CCP	B	2.920	1.247	3.014	1.275	−0.094	−0.028
	bb···π	BCP	C6–Cβ	3.704	1.271	–	–	3.704	1.271
			C6–Hβ	–	–	3.696	1.224	−3.696	−1.224
G–TYR 2'- deoxyribose C2'-side	π···π	BCP	N9–O1	3.676	1.634	3.610	1.612	0.066	0.022
		BCP	C5–C1	5.231	1.485	5.228	1.485	0.003	0.000
		BCP	C6–C2	4.855	1.704	4.866	1.696	−0.011	0.008
		BCP	N1–C4	5.090	1.476	5.090	1.475	0.000	0.000
		BCP	N3–C6	5.159	1.529	5.162	1.528	−0.003	0.002
		CCP	A	3.112	1.359	3.117	1.360	−0.005	−0.001
	bb···π	BCP	C2'–O1	1.944	0.828	1.908	0.797	0.035	0.032
		CCP	B	4.383	2.032	–	–	4.383	2.032
T–TRP' 2'- deoxyribose C2'-side	π···π	BCP	C6–C2	3.747	1.422	3.748	1.418	−0.001	0.004
		BCP	C2–C6	3.988	1.407	3.982	1.412	0.007	−0.005
		BCP	N3–C7	4.036	1.277	4.005	1.259	0.031	0.018
		BCP	C5–C8	5.417	1.410	5.433	1.408	−0.017	0.002
		BCP	C5Me–C9	6.612	2.237	6.612	2.239	0.000	−0.003
		CCP	A	2.889	1.258	2.896	1.259	−0.006	−0.001
		CCP	B	2.848	1.223	2.816	1.211	0.033	0.012
	bb···π	BCP	C2'Ha–H7	5.502	2.056	5.552	2.068	−0.050	−0.011
		BCP	C2'Hb–H8	2.514	0.908	2.485	0.895	0.029	0.013
		CCP	C	1.792	0.722	–	–	1.792	0.722
		CCP	D	5.550	2.565	–	–	5.550	2.565
U–TYR' 2'- deoxyribose O4'-side	π···π	BCP	C4–O1	6.277	2.317	6.449	2.339	−0.172	−0.022
		BCP	N3–C2	7.655	2.104	7.728	2.088	−0.073	0.016
		BCP	N1–C4	7.216	2.025	7.233	2.026	−0.016	−0.001
		BCP	C5–C6	7.789	2.035	7.788	2.036	0.001	−0.001
		CCP	A	4.545	1.812	4.558	1.811	−0.013	0.001
		CCP	B	4.451	1.782	4.437	1.774	0.014	0.008
	bb···π	BCP	O4'–H1	7.897	3.150	7.893	3.151	0.004	−0.001
		BCP	O4'–H2	4.006	1.628	3.934	1.613	0.072	0.015
		CCP	C	3.542	1.675	–	–	3.542	1.675
		CCP	D	5.508	2.547	–	–	5.508	2.547

[a] Bond critical points are labeled with both atoms involved in bonding, where the first atom belongs to the nucleobase and the second atom belongs to the amino acid. See Fig. ESI-4 for atomic numbering. Cage critical points either lay in a plane between the nucleobase and amino acid ring atoms or near the backbone atoms in the deoxyribose sugar backbone, and are distinguished by capitol letters in the molecular graphs (Figs. ESI-1 – ESI-3).

Table ESI-2 The effect of truncated (C_s) and extended (C_1) monomers on $\pi\cdots\pi$ interaction energies.

	Dimer	ΔE_{trunc}[a]	$\Delta E_{\pi\cdots\pi}$[b]	Truncated (C_s) Monomers in Extended Model Geometry[c]	Extended (C_1) $\pi\cdots\pi$ Monomers in Truncated Geometry[d]
Protein Backbone	A–TRP′	-35.0	-37.1	-36.8	-35.2
	G–TRP	-42.4	-44.9	-44.1	-43.1
Deoxyribose Sugar (C2′ side)	A–HIS′	-27.2	-31.5	-26.7	-31.5
	G–HIS′	-31.4	-34.3	-32.5	-33.0
Deoxyribose Sugar (O4′ side)	A–TRP	-32.0	-34.3	-30.7	-33.4
	G–HIS	-35.3	-41.8	-33.2	-40.5

[a] ΔE_{trunc} corresponds to the interaction energy of the most stable geometry determined by potential energy surface scans between truncated (C_s) monomers. [b] $\Delta E_{\pi\cdots\pi}$ corresponds to the interaction energy of the most stable geometry determined by potential energy surface scans between extended (C_1) monomers, where the backbone was removed and replaced by an H atom (whose position was optimized while all other atoms were fixed). [c] The interaction energy calculated using truncated (C_s) monomers in the most stable geometry determined by potential energy surface scans of extended (C_1) monomers. [d] The interaction energy calculated using extended (C_1) monomers (where the backbone was removed and replaced by an H atom (whose position was optimized while all other atoms were fixed)) in the most stable geometry determined by potential energy surface scans of truncated (C_s) monomers.
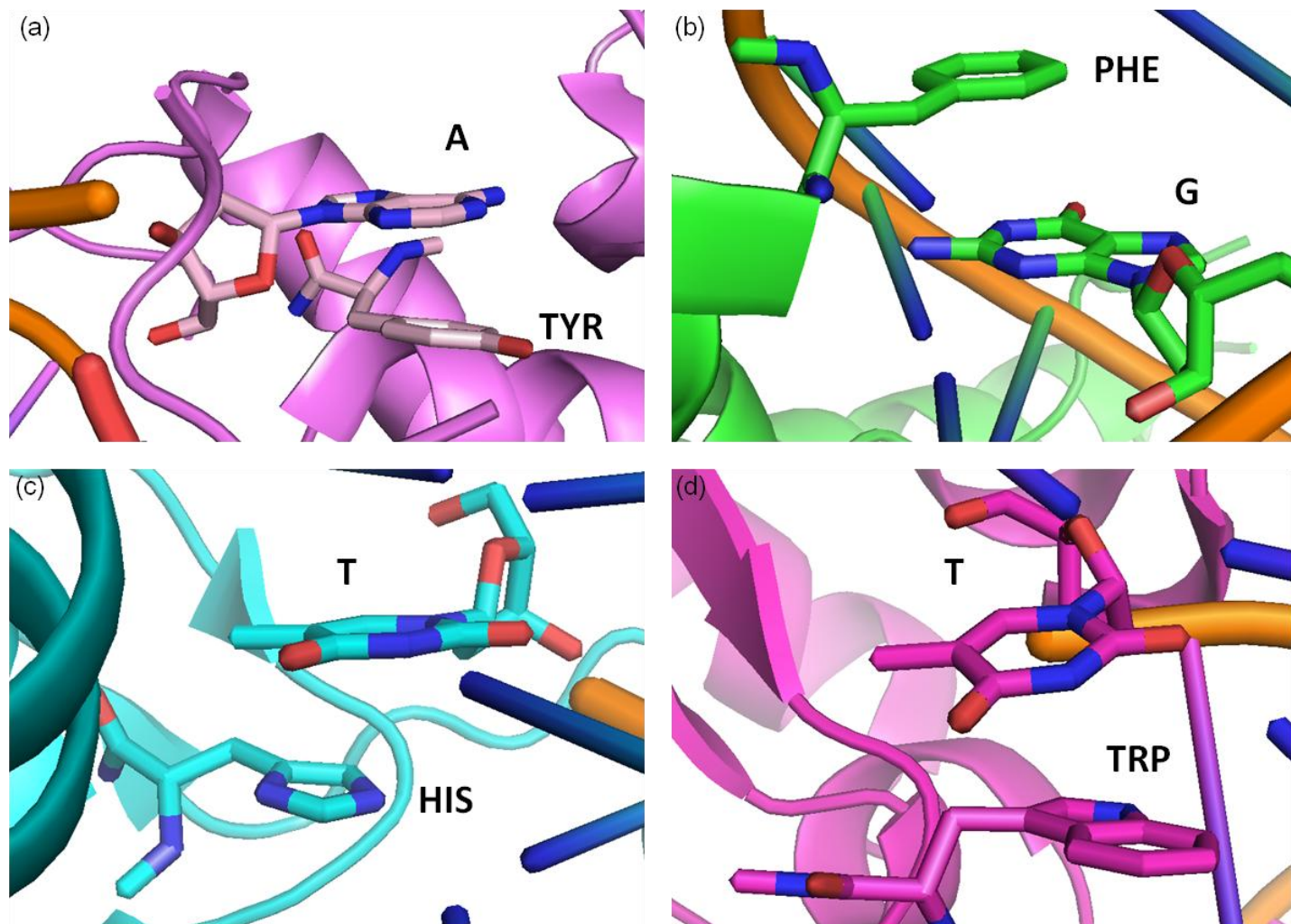
Fig. ESI-5 DNA-protein stacking interactions and the attached biological backbones observed in nature for (a) 1G38[1] (DA606 and Y108), (b) 1CKT[2] (DG109 and F37), (c) 1A1I[3] (DT5 and H149) and (d) 1CW0[4] (DT354 and W68). For each crystal structure, two interactions were considered: 1) a truncated nucleoside (nucleobase) stacked with an extended amino acid; and 2) a nucleoside (extended nucleobase) stacked with a truncated amino acid.

1.   K. Goedecke, M. Pignot, R. S. Goody, A. J. Scheidig and E. Weinhold, *Nat. Struct. Biol.*, 2001, **8**, 121-125.
2.   U. M. Ohndorf, M. A. Rould, Q. He, C. O. Pabo and S. J. Lippard, *Nature*, 1999, **399**, 708-712.
3.   M. Elrod-Erickson, T. E. Benson and C. O. Pabo, *Struct. Fold. Des.*, 1998, **6**, 451-464.
4.   S. E. Tsutakawa, H. Jingami and K. Morikawa, *Cell*, 1999, **99**, 615-623.